

Self-Generation of Fundamental Dark Solitons in Magnetic Films

Boris A. Kalinikos,* Mark M. Scott, and Carl E. Patton†

Department of Physics, Colorado State University, Fort Collins, Colorado 80523
(Received 23 December 1999)

The self-generation of single, fundamental, stable, spin-wave-envelope black and gray dark solitons has been realized for the first time. These solitons were generated from microwave magnetostatic surface waves (MSSWs) propagated in an in-plane magnetized yttrium iron garnet film MSSW delay line in a resonant ring. These fundamental dark solitons were made possible by a new and general filtering technique for a high gain nonlinear resonant ring. The amplitude and phase profiles together with the power spectra of the self-generated microwave pulses confirm their fundamental dark soliton nature.

PACS numbers: 75.30.Ds, 76.50.+g, 85.70.Ge

Two different types of envelope solitons, *bright solitons* and *dark solitons*, can propagate in nonlinear waveguiding dispersive media. Bright and dark solitons may be classified as dynamical and topological, respectively. The term “dynamic” for bright solitons means that these pulses are essentially nonlinear wave packets for which the carrier signal maintains a constant phase over the pulse. The term “topological” denotes the fact that the passage of a single dark soliton modifies the medium or the medium response in some critical way. Dark envelope solitons may be described in terms of a carrier signal of constant amplitude which has a dip in amplitude at the soliton position. If this dip goes completely to zero, one has a *black soliton*. If the minimum power at the dip is nonzero, one has a *gray soliton*. Dark envelope solitons have a nonzero jump in phase for the carrier signal as one crosses the dip. In the case of black solitons, this jump in phase is exactly 180° .

The main experimental results on envelope solitons in solid state media have been for optical solitons in fibers and microwave magnetic envelope (MME) solitons in ferrite films. References [1–3] provide reviews of general properties and optical soliton results. Optical dark solitons are considered specifically in Ref. [4]. References [5–14] are representative of work on MME solitons. Dark MME solitons are considered in Refs. [6,12–14]. Dark MME solitons may be created from cw input signals by switching off the input signal for a short time [6]. In the case of dark MME solitons, however, they must be produced in pairs [12,13]. This is because the jump in phase across a single dark MME soliton is nonzero, while the total phase change for the output signal must be zero.

Because of these phase constraints, the *single fundamental* dark MME soliton has been an entirely theoretical concept. This Letter reports the first experimental demonstration of the self-generation of MME *dark single soliton* pulses, namely, *black single soliton* trains as well as *gray single soliton* trains. These solitons are produced, moreover, through a new technique which is of general validity and not limited to nonlinear microwave signals in magnetic films. One need apply only the proper filtering characteristic to a comb of frequencies obtained through feedback in a nonlinear system under conditions of high gain and

the correct nonlinear response. This technique produces fundamental solitons without the use of input pulse signals or feedback modulation. The experimental proof for single dark solitons is contained in the phase profiles for the pulses. Each dark pulse is accompanied by the expected jump in phase, 180° for black solitons and less for gray solitons.

These new excitations were produced with the resonant ring arrangement shown in Fig. 1. The feedback circuit is shown in the dashed line box. The ring contains the yttrium iron garnet (YIG) film delay line, an amplifier, and an attenuator. The shaded rectangle indicates the YIG film. The input and output microstrip lines connect to the special two element microstrip antennas A_{in} and A_{out} used for excitation and detection. The magnetic field H is in the plane of the film and perpendicular to the magnetostatic wave propagation direction. This is the magnetostatic surface wave (MSSW) configuration. For this arrangement, the nonlinear frequency response and the dispersion have the same sign and combine to support dark MME solitons in the film [6].

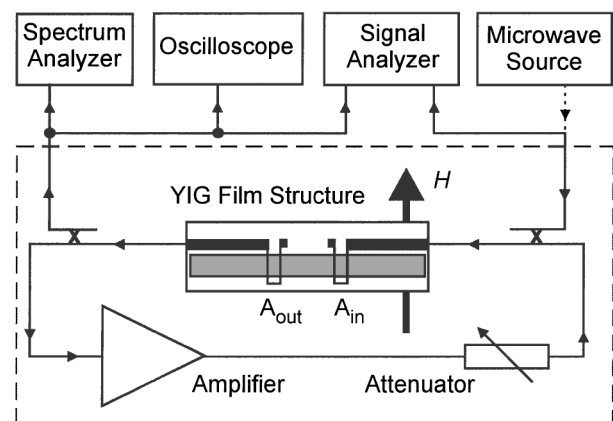


FIG. 1. Diagram of the YIG film delay line structure with two element input and output antennas labeled A_{in} and A_{out} , the in-plane magnetic field H perpendicular to the propagation direction, the resonant ring feedback circuit, and associated instrumentation for the generation of single black and gray solitons. The resonant ring consists of the elements within the dashed line box.

The microwave instrumentation is shown at the top of the figure. The microwave source was used only to measure the passband characteristics of the delay line and the ring at low power, and as a reference for the soliton phase profile measurements. It was not an essential element for soliton generation.

The key difference between this experiment and those in Refs. [10–13] is in the two element microstrip antennas used for MSSW signal excitation and detection. This antenna design provides the filtering response needed to produce solitons. The ring contains *none* of the switching or modulating elements which were used to produce soliton trains in Refs. [10–12].

The YIG film was a $6.9 \mu\text{m}$ thick, 1.4 mm wide, 55 mm long strip cut from a larger film grown by liquid phase epitaxy. This film had unpinned surface spins and a narrow ferromagnetic resonance linewidth. Each antenna element was $50 \mu\text{m}$ wide and 2 mm long. The separation between the two elements for one antenna was 0.26 mm . The separation L between the two antennas was 2 mm . The microwave amplifier had a bandwidth greater than 5 GHz , a 30 dB dynamic range, and a high peak power. This ensured that the nonlinear response of the ring was determined solely by the YIG film.

Figure 2 shows three output power vs frequency response profiles. These data were obtained for $H = 970 \text{ Oe}$, a low level input microwave power of about -30 dBm , and

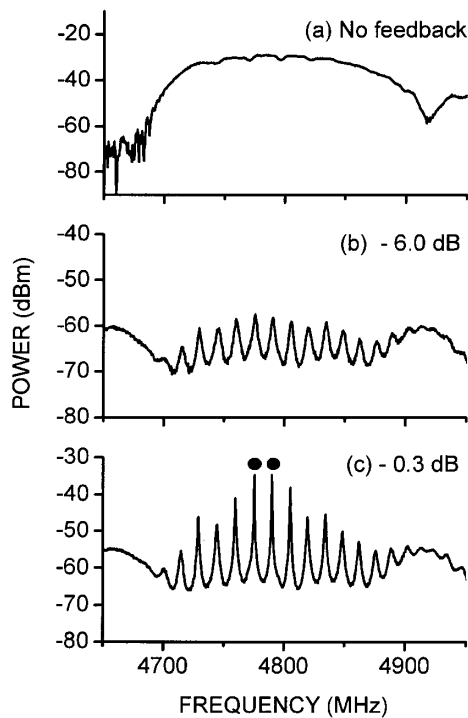


FIG. 2. Frequency characteristics of the MSSW YIG film structure and resonant ring for an input power of about -30 dBm . The nominal static magnetic field was 970 Oe . The applicable ring gains in dB are indicated. The black dots in (c) identify the two largest ring resonance spikes.

ring gains as indicated. The zero dB gain point, or unity gain, was determined as the point at which the ring would just break into oscillation. Graph (a) of Fig. 2 shows the response of the YIG film delay line alone. Graphs (b) and (c) of Fig. 2 show the effect of feedback on the response.

The profile in Fig. 2(a) is typical of the delay line response for MSSW excitations [15], but with a reduced bandwidth due to the two element antenna response. The MSSW passband starts for signals at zero wave number at about $4660\text{--}4670 \text{ MHz}$. As the frequency increases from this point, the wave number k increases. The upper edge of the passband near 4920 MHz corresponds to the point in k at which the MSSW signals from the two elements of the antenna are out of phase by 180° . This passband was made slightly broader than the expected width of the single soliton power frequency spectrum, in order to enhance the conditions for soliton formation.

The well defined spikes in Figs. 2(b) and 2(c) correspond to the resonant frequencies of the ring. At these spike points, the phase matching condition $kL + \phi = 2\pi n$ is satisfied, where kL is the phase change for the delay line, ϕ is the electronic phase associated with the rest of the ring, and n is any integer. The spike spacing is about 14.6 MHz . The envelope of these spikes is just the two element antenna filter response in Fig. 2(a). The two spikes in Fig. 2(c) which are identified with black dots are right at the passband center and have equal amplitudes. The next spike to the right is lower by about 3 dB . Since the feedback threshold for oscillation in the ring is determined by the spikes with the highest power level, the two equal amplitude spikes will dominate any linear self-oscillation response. At high ring gain, these spikes provide the seed response for the formation of fundamental dark solitons. The filtered MSSW passband and the nonlinear MSSW modulational instability response combine to shape the spectral response to produce such solitons.

Because of the MSSW dispersion, small changes in field can serve to shift the relative position of the comb of spikes in Fig. 2(c) relative to the passband. Such field tuning can be used to change the relative heights of the dominant spikes in the power spectrum. Equal spike amplitudes provide the seed response needed to produce black solitons. If the dominant spikes have different amplitudes, one obtains gray solitons. The details involve the selective high level response for two closely spaced frequencies. If the ring gain is sufficient to produce self-oscillation, the seed response and the nonlinear response of the MSSW signals combine to produce trains of the appropriate solitons.

As a starting point, consider two equal amplitude propagating cw signals with different frequencies f_1 and f_2 . The combination of these signals yields a nonzero background with dips to zero amplitude at the beat points. The beat repetition period T is $1/|f_1 - f_2|$. There is also a carrier phase jump of 180° across each dip. The pulse sequence produced by the interference of these two signals, therefore, can provide the seed response for a train of single

fundamental dark solitons. As indicated above, small changes in the field could cause an imbalance in these two equal amplitude signals. One still obtains dips at the repetition period T given above. Now, however, the dips do not go to zero amplitude and the phase jumps across the dips are less than 180° . This is the seed response for gray solitons.

The procedure outlined above was used to produce both black and gray fundamental dark solitons. For black solitons, the structure was first configured to produce the response shown in Fig. 2(c) with the two largest ring resonance spikes at equal amplitude. The gain was then increased to the point needed to (i) produce a self-generated microwave response in the circuit and (ii) allow the nonlinear process to develop. The result was a narrowing of the envelope response to yield the cusplike dips characteristic of fundamental black solitons.

Figure 3 shows representative black soliton results. These data were obtained for a ring gain of $+0.5$ dB and the other conditions as specified above. Except for the phase data, these results are representative of data obtained with no microwave input signal whatsoever. A low level microwave reference at 4785 MHz was used for the phase measurements. The power level for this reference signal was 35 dB below the power levels for the self-generated frequency harmonics in the ring. Care was taken to ensure that this reference did not affect the ring signal response in any way. The top four graphs show the experimental black soliton amplitude and phase profiles, respectively. The voltage levels indicated were measured at the signal analyzer. The dashed line curve in (a-e) of Fig. 3 shows

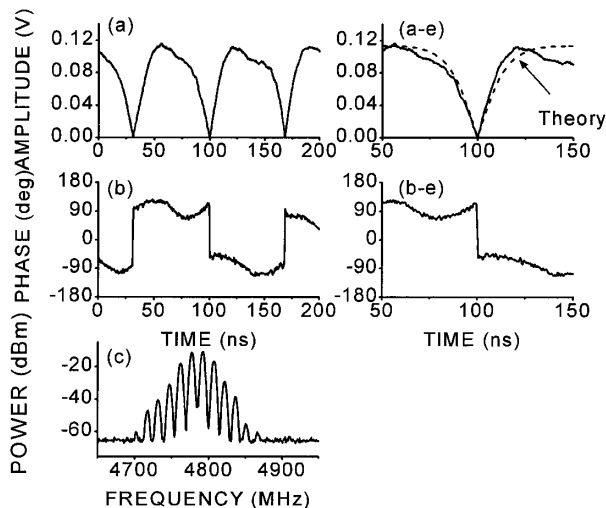


FIG. 3. Fundamental black soliton pulse train characteristics. Graphs (a) and (b) show the microwave voltage and phase profiles, respectively, for the self-generated signal in the ring structure with a ring gain of $+0.5$ dB. Graphs (a-e) and (b-e) show the same signals as in (a) and (b) but on an expanded time scale. The dashed curve in (a-e) shows a theoretical profile. Graph (c) shows the corresponding power-frequency spectrum of the ring signal.

a theoretical amplitude profile as well. The bottom graph shows the power frequency spectrum for the measured signals.

The signal characteristics for these data match those expected for single black solitons. The cusps in (a) and (a-e) of Fig. 3 are sharp and distinct and fall precisely to zero at the pulse center. The data in (b) and (b-e) of Fig. 3 also show the 180° jumps in phase across the dips expected from theory. The power spectrum in Fig. 3(c) shows multiple harmonics over a bandwidth which is narrower than the passband in Fig. 2. Note that the two primary peaks in Fig. 3(c) have equal amplitudes. Note also that the self-generated black soliton sequence has a power-frequency spectrum with peaks which coincide with the cw resonance frequencies of the ring. The 14.6 MHz spacing in the frequency peaks corresponds to a repetition period of 68.5 ns. This value matches the observed repetition period for the black soliton train in (a) and (b) of Fig. 3.

It is to be emphasized that these signals consist of trains of single isolated fundamental black solitons, not the double cusp dips which have been previously reported for pairs of dark solitons [12,13]. It is also to be emphasized that these fundamental soliton signals were obtained with no external microwave signal applied to the ring. These single black solitons were self-generated solely through the nonlinear feedback process within the ring. The 180° phase jumps at the dip positions give an unambiguous signature for black solitons.

Figure 4 shows representative data on gray soliton self-generation. The conditions were the same as for the data in Fig. 3, except that the static magnetic field was reduced from 970 to 968 Oe. This small change served to imbalance the amplitudes of the two dominant spikes in the power spectrum of Fig. 2(c), and this imbalance gave the seed signal needed for gray solitons. The format for Fig. 4 is the same as for Fig. 3, except that here both graphs (a-e) and (b-e) show theoretical profiles.

The gray soliton data show different characteristics compared to the Fig. 3 data. (i) The dips in amplitude do not go to zero. (ii) The dips are more rounded and less cusplike, compared to the black solitons. (iii) The phase changes around each dip are no longer abrupt. (iv) The overall phase change associated with a given dip is smaller than 180° . (v) The two main peaks in the power spectrum are slightly imbalanced. The features shown in Fig. 4 are those expected for gray solitons. The particular data in Fig. 4 show phase changes for each dip of about 150° . The width of the gray soliton dips was also found to change with the ring gain setting. Higher gains yielded somewhat narrower widths.

The dark soliton response characteristics shown in Figs. 3 and 4 could be maintained only over a limited 1 dB or so range of gain settings. When the gain in the ring is increased much above the $+0.5$ dB value used for the above data, the amplitude and phase profiles become distorted and the power-frequency spectrum is also modified.

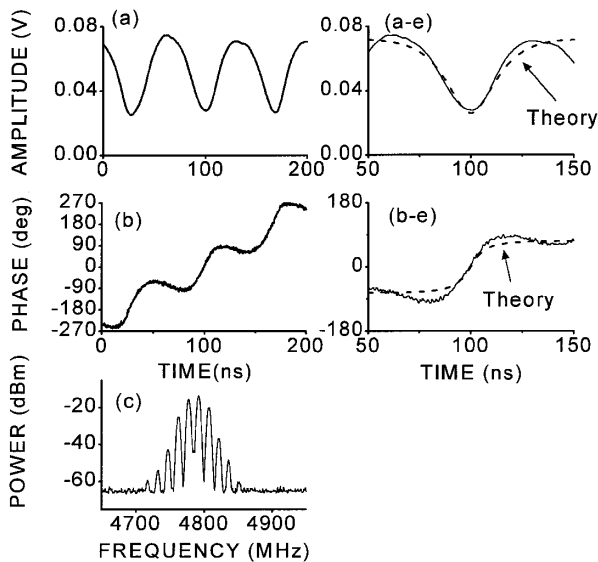


FIG. 4. Gray soliton pulse train characteristics. Graphs (a) and (b) show the detected microwave voltage and phase profiles, respectively, for the self-generated signal in the ring structure for a gain of +0.5 dB. Graphs (a-e) and (b-e) show the same signals as in (a) and (b) but on an expanded time scale. The dashed curves in (a-e) and (b-e) show theoretical profiles. Graph (c) shows the corresponding power-frequency spectrum of the ring signal.

With an increase of the gain factor above the stable soliton self-generation range, the power spectra showed a series of bifurcations and the onset of chaotic behavior. These features of the response at high gain levels require further study. In addition to the achievement of fundamental dark soliton generation, the technique has potential applications to the study of chaos in these systems.

The dashed curves in Figs. 3 and 4 were obtained from the standard dark soliton amplitude and phase solutions to the nonlinear Schrödinger (NLS) equation [3], based on values for the dispersion and nonlinear coefficients and the modulation levels appropriate to the data. For the black soliton curves, the theoretical background level off-soliton response was obtained from the measured width of the cusp and this background level was scaled to the data. For the gray soliton response, the modulation level shown by the data was used to calculate the theoretical response and this was then scaled to match the data. The fits show that the simple NLS equation dark soliton solutions provide a reasonable match to the data. It may be noteworthy that this match is obtained without the inclusion of damping in the model. The NLS equation with damping included has been shown to provide an accurate model for bright MME solitons in YIG films [16].

In summary, this Letter reports on the first self-generation of isolated, single, fundamental dark microwave magnetic envelope solitons. The filtered feedback technique is shown to provide a powerful way to self-generate such fundamental dark signals, even though the phase con-

straints imposed on fundamental dark solitons preclude their creation from conventional input microwave signals. The combination of a properly devised filtering response for the MSSW signal, feedback in the resonant ring structure, and the modulational instability which derives from the nonlinear response make possible the creation of such fundamental dark soliton signals. This technique represents a completely new approach to dark soliton production in general for nonlinear dispersive waveguiding media.

Dr. V. T. Synogach is acknowledged for assistance with the experiment. This work was supported in part by the U.S. Army Research Office, Grant No. DAAG55-98-1-0430, the National Science Foundation, Grant No. DMR-9801649, the Russian Foundation for Basic Research, Grant No. 99-02-16370, the NATO Linkage Grant Program, Grant No. HTECH.LG 970538, and the Alexander von Humboldt Foundation.

*Permanent address: St. Petersburg Electrotechnical University, 197376 St. Petersburg, Russia.

†On sabbatical leave at the Fachbereich Physik, Universität Kaiserslautern, Kaiserslautern, D-67663, Germany.

- [1] *Optical Solitons—Theory and Experiment*, edited by J. R. Taylor (Cambridge University Press, Cambridge, England, 1992).
- [2] G. P. Agrawal, *Nonlinear Fiber Optics* (Academic Press, San Diego, 1995).
- [3] M. Remeissenet, *Waves Called Solitons: Concepts and Experiments* (Springer-Verlag, Berlin, 1996).
- [4] Y. S. Kivshar and B. Luther-Davies, *Phys. Rep.* **298**, 81 (1998).
- [5] B. A. Kalinikos, N. G. Kovshikov, and A. N. Slavin, *Zh. Eksp. Teor. Fiz.* **94**, 159 (1988) [*Sov. Phys. JETP* **67**, 303 (1988)].
- [6] M. Chen, M. A. Tsankov, J. M. Nash, and C. E. Patton, *Phys. Rev. Lett.* **70**, 1707 (1993).
- [7] M. Chen, M. A. Tsankov, J. M. Nash, and C. E. Patton, *Phys. Rev. B* **49**, 12773 (1994).
- [8] R. Marcelli and P. De Gasperis, *IEEE Trans. Magn.* **30**, 26 (1994).
- [9] J. M. Nash, C. E. Patton, and P. Kabos, *Phys. Rev. B* **51**, 15079 (1995).
- [10] B. A. Kalinikos, N. G. Kovshikov, and C. E. Patton, *Phys. Rev. Lett.* **78**, 2827 (1997).
- [11] B. A. Kalinikos, N. G. Kovshikov, and C. E. Patton, *Phys. Rev. Lett.* **80**, 4301 (1998).
- [12] B. A. Kalinikos, N. G. Kovshikov, and C. E. Patton, *Pis'ma Zh. Eksp. Teor. Fiz.* **68**, 229 (1998) [*JETP Lett.* **68**, 243 (1998)].
- [13] B. A. Kalinikos, N. G. Kovshikov, and C. E. Patton, *Appl. Phys. Lett.* **75**, 265 (1999).
- [14] A. N. Slavin, Y. S. Kivshar, E. A. Ostrovskaya, and H. Benner, *Phys. Rev. Lett.* **82**, 2583 (1999).
- [15] R. W. Damon and J. R. Eshbach, *J. Phys. Chem. Solids* **19**, 308 (1961).
- [16] H. Y. Zhang, P. Kabos, H. Xia, R. A. Staudinger, P. A. Kolodin, and C. E. Patton, *J. Appl. Phys.* **84**, 3776 (1998).